Journal of Nanofluids
Vol. 3, pp. 65–71, 2014
(www.aspbs.com/jon)

Natural Convective Boundary Layer Flow Over a Vertical Cone Embedded in a Porous Medium Saturated with a Nanofluid

Rama Subba Reddy Gorla[1,*], Ali Chamkha[2], and Kaustubh Ghodeswar[1]

[1] *Cleveland State University, Cleveland, Ohio 44115, USA*
[2] *Public Authority for Applied Education and Training, Shuweikh 70654, Kuwait*

A boundary layer analysis is presented for the natural convection past a non-isothermal vertical cone in a porous medium saturated with a nanofluid. Numerical results for friction factor, surface heat transfer rate and mass transfer rate have been presented for parametric variations of the buoyancy ratio parameter N_r, Brownian motion parameter N_b, thermophoresis parameter N_t and Lewis number Le. The dependency of the friction factor, surface heat transfer rate (Nusselt number) and mass transfer rate (Sherwood number) on these parameters has been discussed.

KEYWORDS: Natural Convection, Porous Medium, Nanofluid.

1. INTRODUCTION

The study of convective heat transfer in nanofluids is gaining a lot of attention. The nanofluids have many applications in the industry since materials of nanometer size have unique physical and chemical properties. Nanofluids are solid–liquid composite materials consisting of solid nanoparticles or nanofibers with sizes typically of 1–100 nm suspended in liquid. Nanofluids have attracted great interest recently because of reports of greatly enhanced thermal properties. For example, a small amount ($< 1\%$ volume fraction) of Cu nanoparticles or carbon nanotubes dispersed in ethylene glycol or oil is reported to increase the inherently poor thermal conductivity of the liquid by 40% and 150%, respectively.[1,2] Conventional particle-liquid suspensions require high concentrations ($> 10\%$) of particles to achieve such enhancement. However, problems of rheology and stability are amplified at high concentrations, precluding the widespread use of conventional slurries as heat transfer fluids. In some cases, the observed enhancement in thermal conductivity of nanofluids is orders of magnitude larger than predicted by well-established theories. Other perplexing results in this rapidly evolving field include a surprisingly strong temperature dependence of the thermal conductivity[3] and a three-fold higher critical heat flux compared with the base fluids.[4,5] These enhanced thermal properties are not merely of academic interest. If confirmed and found consistent, they would make nanofluids promising for applications in thermal management. Furthermore, suspensions of metal nanoparticles are also being developed for other purposes, such as medical applications including cancer therapy. The interdisciplinary nature of nanofluid research presents a great opportunity for exploration and discovery at the frontiers of nanotechnology.

Porous media heat transfer problems have several engineering applications such as geothermal energy recovery, crude oil extraction, ground water pollution, thermal energy storage and flow through filtering media. Cheng and Minkowycz[6] presented similarity solutions for free convective heat transfer from a vertical plate in a fluid-saturated porous medium. Gorla and co-workers[7,8] solved the nonsimilar problem of free convective heat transfer from a vertical plate embedded in a saturated porous medium with an arbitrarily varying surface temperature or heat flux. The problem of combined convection from vertical plates in porous media was studied by Minkowycz et al.[9] and Ranganathan and Viskanta.[10] All these studies were concerned with Newtonian fluid flows. The boundary layer flows in nanofluids have been analyzed recently by Nield and Kuznetsov and Kuznetsov[11] and Nield and Kuznetsov.[12] A clear picture about the nanofluid boundary layer flows is still to emerge. Kumari and Jayanthi[13] considered the effect of uniform lateral mass flux on the natural convection flow on a vertical cone in a porous medium saturated with power-law fluid. Kumari and Nath[14] presented an analysis for the non-Darcy natural convection flow of a Newtonian fluid due to the combined action of heat and mass diffusion on a vertical cone in a porous

*Author to whom correspondence should be addressed.
Email: r.gorla@csuohio.edu
Received: 12 July 2013
Accepted: 29 July 2013

ARTICLE

medium. Prabhat et al.[15] discussed the enhancement in heat transfer by using nanofluids. Murshed et al.[16] formulated a Brownian motion-based model for the prediction of the thermal conductivity of nanofluids. Murshed et al.[17] investigated the effect of surfactant and nanoparticle clustering on thermal conductivity of nanofluids. Calvin et al.[18] analyzed the dual role of nanoparticles on thermal conductivity enhancement of nanofluids.

The present work has been undertaken in order to analyze the natural convection past a vertical cone embedded in a porous medium saturated by a nanofluid. The effects of Brownian motion and thermophoresis are included for the nanofluid. Numerical solutions of the boundary layer equations are obtained and discussion is provided for several values of the nanofluid parameters governing the problem.

2. ANALYSIS

We consider the steady free convection boundary layer flow past a vertical cone with semi-vertical angle $\boldsymbol{\Omega}$ placed in a nano-fluid saturated porous medium. The co-ordinate system is selected such that x-axis is aligned with slant surface of the cone, as shown in Figure 1.

We consider the axi-symmetric problem. We consider at $y = 0$, the temperature T and the nano-particle fraction ϕ take constant values T_W and ϕ_W, respectively. The ambient values, attend as y tends to infinity, of T and ϕ are denoted by T_∞ and ϕ_∞, respectively. The Oberbeck-Boussinesq approximation is employed. Homogeneity and local thermal equilibrium in the porous medium is assumed.

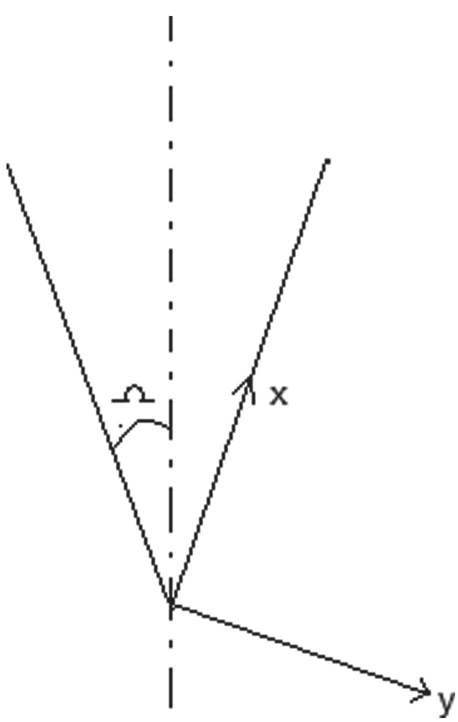

Fig. 1. Flow model and coordinate system.

We consider the porous medium whose porosity is denoted by ε and permeability by K.

We now make the standard boundary layer approximation based on a scale analysis and write the governing equations.

$$\frac{\partial}{\partial x}(ru) + \frac{\partial}{\partial y}(rv) = 0 \tag{1}$$

$$\frac{\partial u}{\partial y} + \frac{\rho_{f\infty} K^*}{\mu} \cdot \frac{\partial}{\partial y}(u^2) = \frac{(1-\phi_\infty)\rho_{f\infty}\beta g K \cos\Omega}{\mu} \cdot \frac{\partial T}{\partial y} - \frac{(\rho_P - \rho_{f\infty}) g K \cos\Omega}{\mu} \cdot \frac{\partial \phi}{\partial y} \tag{2}$$

$$u \cdot \frac{\partial T}{\partial x} + v \cdot \frac{\partial T}{\partial y} = \alpha_m \frac{\partial^2 T}{\partial y^2} + \tau\left[D_B \frac{\partial \phi}{\partial y}\frac{\partial T}{\partial y} + \frac{D_T}{T_\infty}\left(\frac{\partial T}{\partial y}\right)^2\right] \tag{3}$$

$$\frac{1}{\varepsilon}\left(u\frac{\partial \phi}{\partial x} + v\frac{\partial \phi}{\partial y}\right) = D_B \frac{\partial^2 \phi}{\partial y^2} + \left(\frac{D_T}{T_\infty}\right)\frac{\partial^2 T}{\partial y^2} \tag{4}$$

Where

$$\alpha_m = \frac{k_m}{(\rho c)_f}, \quad \tau = \frac{\varepsilon(\rho c)_p}{(\rho c)_f} \tag{5}$$

Here ρ_f, μ and β are the density, viscosity and volumetric volume expansion coefficient of the fluid while ρ_p is the density of the particles. The gravitational acceleration is denoted by g. We have introduced the effective heat capacity $(\rho c)_m$ and effective thermal conductivity k_m of the porous medium. The coefficients that appear in Eqs. (3) and (4) are the Brownian diffusion coefficient D_B and the thermophoretic diffusion coefficient D_T.

The boundary conditions are taken to be

$$v = 0, \quad T = T_W, \quad \phi = \phi_W, \quad \text{at } y = 0 \tag{6}$$

$$u = v = 0, \quad T \to T_\infty, \quad \phi \to \phi_\infty, \quad \text{as } y \to \infty \tag{7}$$

We introduce a stream line function ψ defined by

$$u = \frac{1}{r}\frac{\partial \psi}{dy}, \quad v = -\frac{1}{r}\frac{\partial \psi}{dx} \tag{8}$$

so that Eq. (1) is satisfied identically. We are then left with the following three equations.

$$\frac{1}{r}\frac{\partial^2 \psi}{\partial y^2} + \frac{\rho_{f\infty} K^*}{\mu} \cdot \frac{\partial}{\partial y}\left(\frac{1}{r}\frac{\partial \psi}{\partial y}\right)^2 = \frac{(1-\phi_\infty)\rho_{f\infty}\beta g K \cos\Omega}{\mu}\frac{\partial T}{\partial y} - \frac{(\rho_P - \rho_{f\infty}) g K \cos\Omega}{\mu}\frac{\partial \phi}{\partial y} \tag{9}$$

$$\frac{1}{r}\frac{\partial \psi}{\partial y}\frac{\partial T}{\partial x} - \frac{1}{r}\frac{\partial \psi}{\partial x}\frac{\partial T}{\partial y} = \alpha_m \frac{\partial^2 T}{\partial y^2} + \tau\left[D_B \frac{\partial \phi}{\partial y}\frac{\partial T}{\partial y} + \left(\frac{D_T}{T_\infty}\right)\left(\frac{\partial T}{\partial y}\right)^2\right] \tag{10}$$

$$\frac{1}{\varepsilon}\left(\frac{1}{r}\frac{\partial \psi}{\partial y}\frac{\partial \phi}{\partial x} - \frac{1}{r}\frac{\partial \psi}{\partial x}\frac{\partial \phi}{\partial y}\right) = D_B \frac{\partial^2 \phi}{\partial y^2} + \left(\frac{D_T}{T_\infty}\right)\frac{\partial^2 T}{\partial y^2} \tag{11}$$

Proceeding with the analysis we introduce the following dimensionless variables:

$$\eta = \frac{y}{x}\cdot Ra_x^{1/2}$$
$$Ra_x = \frac{(1-\phi_\infty)\rho_{f\infty}\beta g K x\cos\Omega(T_W - T_\infty)}{\mu\cdot\alpha_m} \qquad (12)$$
$$S = \frac{\psi}{\alpha_m\cdot r\cdot Ra_x^{1/2}} \quad \theta = \frac{T-T_\infty}{T_W-T_\infty} \quad f = \frac{\phi-\phi_\infty}{\phi_W-\phi_\infty}$$

We assume that

$$\xi = x/L \quad r = x\sin\Omega$$

where, L is the slant height of cone having apex angle of 2Ω.

Substituting the expressions in Eq. (12) into the governing Eqs. (9)–(11) we obtain the following transformed equations:

$$S''(1+A\cdot S') - \theta' + N_r\cdot f' = 0 \qquad (13)$$
$$\theta'' + \frac{3}{2}S\theta' + N_b\cdot f'\cdot\theta' + N_t(\theta')^2 = 0 \qquad (14)$$
$$f'' + \frac{3}{2}\mathrm{Le}\cdot S\cdot f' + \frac{N_t}{N_b}\theta'' = 0 \qquad (15)$$

where the parameters are defined as:

$$N_r = \frac{(\rho_P - \rho_{f\infty})(\phi_W-\phi_\infty)}{\rho_{f\infty}\beta(T_W-T_\infty)(1-\phi_\infty)}$$
$$N_b = \frac{\varepsilon(\rho c)_P D_B(\phi_W-\phi_\infty)}{(\rho c)_f\alpha_m}$$
$$N_t = \frac{\varepsilon(\rho c)_P D_T(T_W-T_\infty)}{(\rho c)_f\alpha_m T_\infty} \qquad (16)$$
$$\mathrm{Le} = \frac{\alpha_m}{\varepsilon\cdot D_B} \quad A = \frac{2\cdot\rho_{f\infty}K^*\alpha_m\cdot Ra_x^{12}}{\mu\cdot x^{1/2}}$$

The transformed boundary conditions are:

$$\eta = 0: \quad S = 0, \quad \theta = 1, \quad f = 1$$
$$\eta\to\infty: \quad S' = 0, \quad \theta = 0, \quad f = 0 \qquad (17)$$

The Heat transfer rate is given by:

$$q_W = -k_f\left.\frac{\partial T}{\partial y}\right|_{y=0}$$

The heat transfer coefficient is given by:

$$h = \frac{q_W}{(T_W - T_\infty)}$$

Local Nusselt number is given by:

$$\mathrm{Nu}_x = \frac{h\cdot x}{k_f} = -Ra_x^{1/2}\cdot\theta'(\xi,0) \qquad (18)$$

The Mass Transfer rate is given by:

$$N_W = -D\left.\frac{\partial\phi}{\partial y}\right|_{y=0} = h_m(\phi_W-\phi_\infty)$$

Where h_m = mass transfer coefficient,

$$N_W = -D\cdot(\phi_W-\phi_\infty)f'\cdot\frac{Ra_x^{1/2}}{x}$$

Sherwood number is given by:

$$Sh = \frac{h_m\cdot x}{D} = -Ra_x^{1/2}\cdot f'(\xi,0) \qquad (19)$$

The local friction factor is given by Cf_x:

$$\tau_W = \mu\cdot\left.\frac{\partial u}{\partial y}\right|_{y=0}$$
$$Cf_x = \frac{\tau_W}{((\rho U^2)/2)} = \frac{2\cdot Ra_x^{3/2}\cdot S''(\xi,0)}{\mathrm{Re}_x^2\cdot\mathrm{Pr}} \qquad (20)$$

3. RESULTS AND DISCUSSION

Equations (13)–(15) were solved numerically to satisfy the boundary conditions (17) for parametric values of Le, N_r

Table I. Effects of N_r on $S''(0)$, $-\theta'(0)$ and $-f'(0)$ for $A=0$, $N_b=0.3$, $N_t=0.1$ and $\mathrm{Le}=10$.

N_r	$S''(0)$	$-\theta'(0)$	$-f'(0)$
0.1	−0.0312865	0.5712565	2.804848
0.2	−0.0019119	0.5582566	2.694939
0.3	0.0251270	0.5453198	2.579612
0.4	0.0493482	0.5310432	2.458157
0.5	0.0706557	0.5160794	2.329314

Table II. Effects of N_t on $S''(0)$, $-\theta'(0)$ and $-f'(0)$ for $A=0$, $N_b=0.2$, $N_r=0.5$, and $\mathrm{Le}=10$.

N_t	$S''(0)$	$-\theta'(0)$	$-f'(0)$
0.1	0.0641585	0.5561268	2.288450
0.2	0.0648676	0.5315452	2.251458
0.3	0.0659185	0.5084322	2.225397
0.4	0.0673317	0.4870419	2.209107
0.5	0.0691260	0.4667582	2.201233

Table III. Effects of N_b on $S''(0)$, $-\theta'(0)$ and $-f'(0)$ for $A=0$, $N_r=0.5$, $N_t=0.3$, and $\mathrm{Le}=10$.

N_b	$S''(0)$	$-\theta'(0)$	$-f'(0)$
0.1	0.0497210	0.5349890	1.981256
0.2	0.0659184	0.5084322	2.225397
0.3	0.0742498	0.4742139	2.311157
0.4	0.0804960	0.4400252	2.356310
0.5	0.0856258	0.4070248	2.385364

ARTICLE

(buoyancy ratio number), N_b (Brownian motion parameter) and N_t (thermophoresis parameter) using finite difference method. Tables I–V indicate results for wall values for the gradients of velocity, temperature and concentration

Table IV. Effects of Le on $S''(0)$, $-\theta'(0)$ and $-f'(0)$ for $A = 0$, $N_b = 0.3$, $N_r = 0.5$, and $N_t = 0.1$.

Le	$S''(0)$	$-\theta'(0)$	$-f'(0)$
1	−0.0247837	0.4542890	0.4505144
10	0.0706557	0.5160794	2.329314
100	0.3713232	0.5359154	7.893836
1000	1.3232000	0.5425866	25.34372

Table V. Effects of A on $S''(0)$, $-\theta'(0)$ and $-f'(0)$ for $N_b = 0.3$, $N_r = 0.5$, $N_t = 0.1$ and Le = 10.

A	$S''(0)$	$-\theta'(0)$	$-f'(0)$
0	0.0706557	0.5160794	2.329314
0.1	0.0664542	0.5092353	2.297508
1.0	0.0447551	0.4670312	2.095359
10	0.0140631	0.3444217	1.532180
100	0.0028694	0.2172511	0.9562534

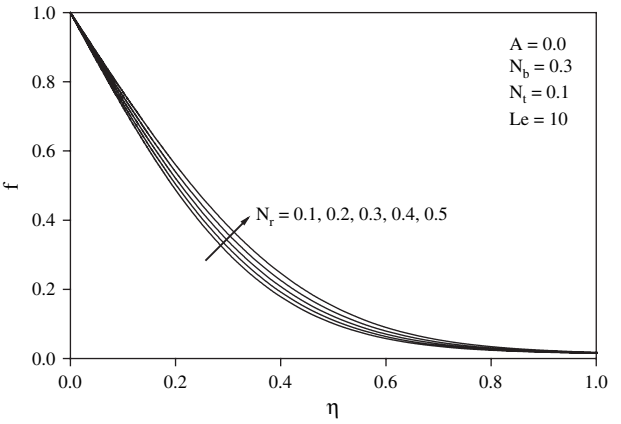

Fig. 4. Effects of N_r on volume fraction profiles.

functions which are proportional to the friction factor, Nusselt number and Sherwood number, respectively. From Tables I–III, we notice that as N_r and N_t increase, the friction factor increases whereas the heat transfer rate (Nusselt number) and mass transfer rate (Sherwood number) decrease. As N_b increases, the friction factor and

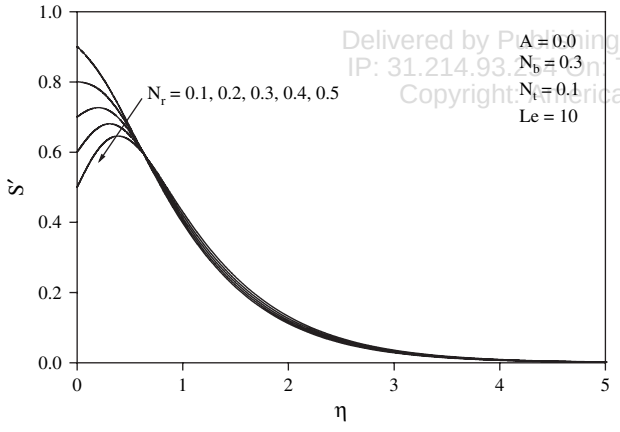

Fig. 2. Effects of N_r on velocity profiles.

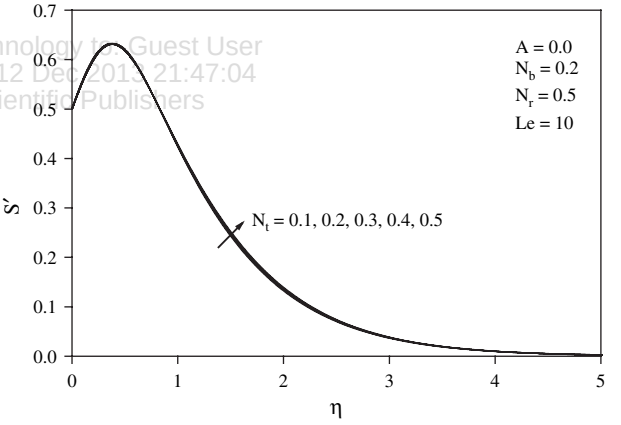

Fig. 5. Effects of N_t on velocity profiles.

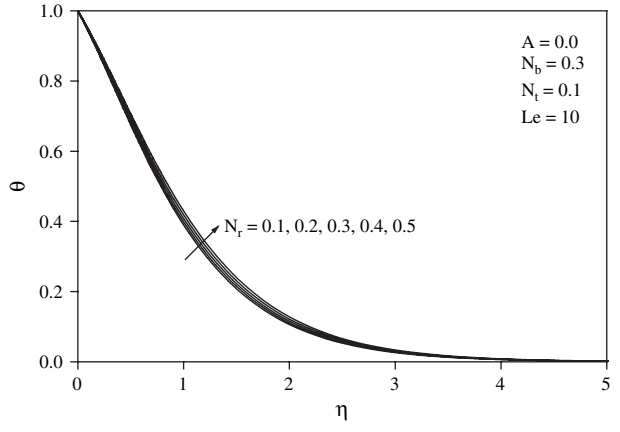

Fig. 3. Effects of N_r on temperature profiles.

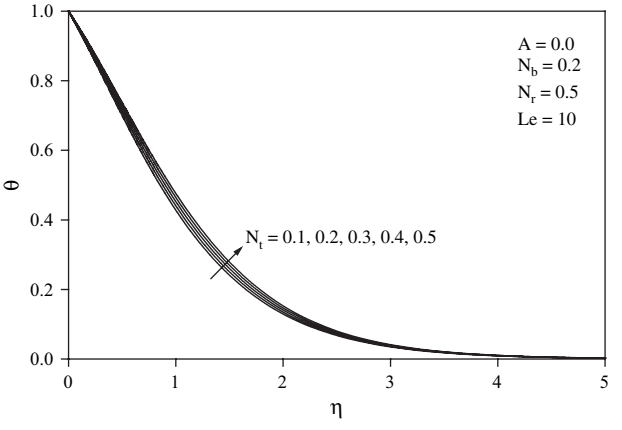

Fig. 6. Effects of N_t on temperature profiles.

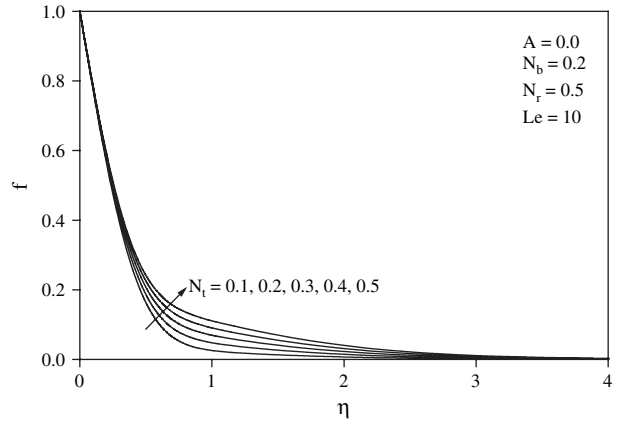

Fig. 7. Effects of N_t on volume fraction profiles.

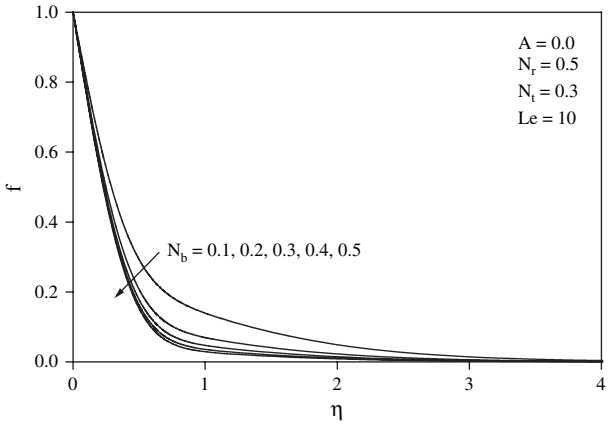

Fig. 10. Effects of N_b on volume fraction profiles.

surface mass transfer rates increase whereas the surface heat transfer rate decreases. Results from Table IV indicate that as Le increases, The heat and mass transfer rates increase. From Table V, we observe that as the non-Darcy parameter A increases, the heat and mass transfer rates decrease.

Figures 2–4 indicate that as N_r increases, the velocity decreases and the temperature and concentration increase. Similar effects are observed from Figures 5–10 as N_t and N_b vary. Figure 11 illustrates the variation of velocity within the boundary layer as Le increases. The velocity increases as Le increases. From Figures 12 and 13, we

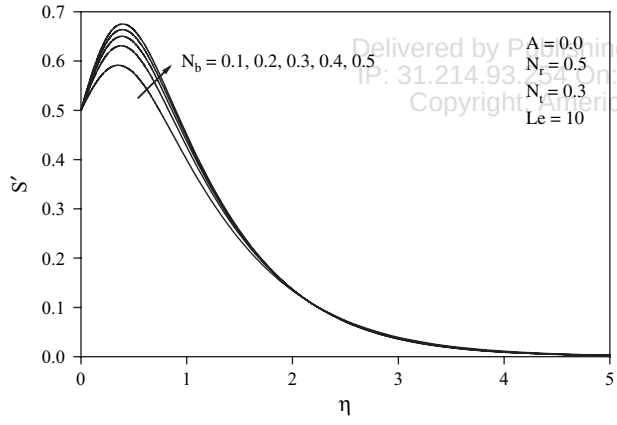

Fig. 8. Effects of N_b on velocity profiles.

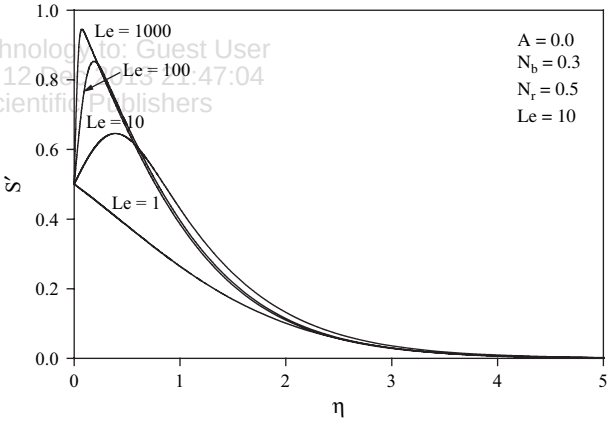

Fig. 11. Effects of Le on velocity profiles.

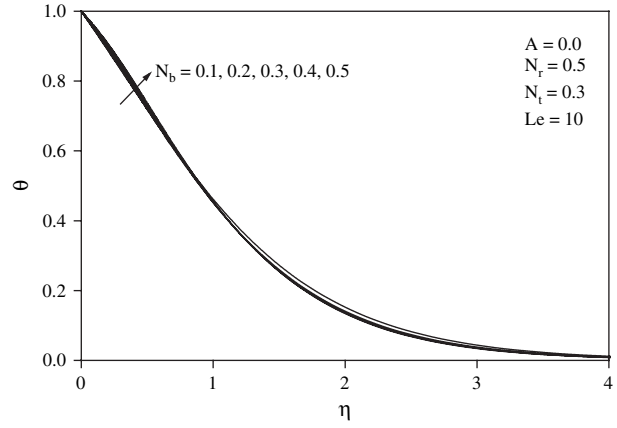

Fig. 9. Effects of N_b on temperature profiles.

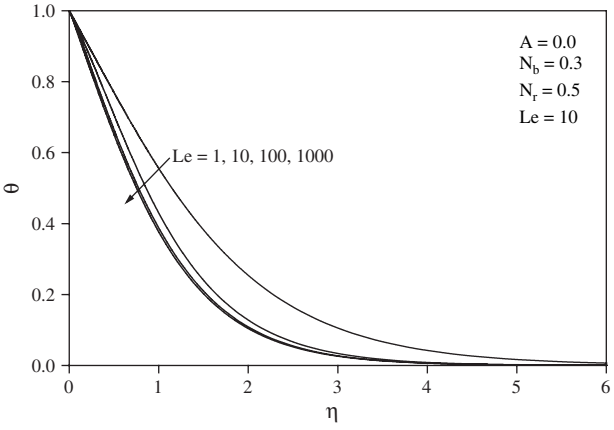

Fig. 12. Effects of Le on temperature profiles.

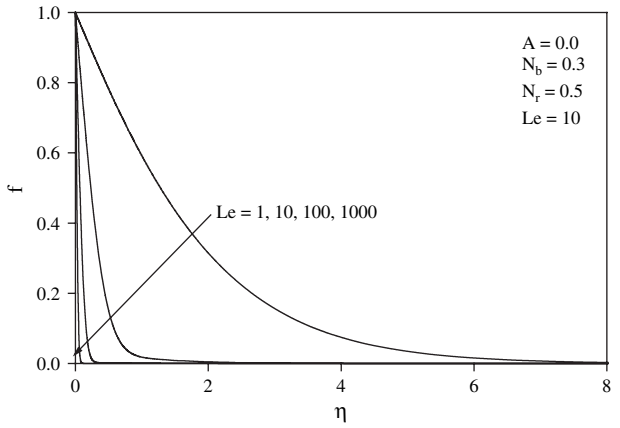

Fig. 13. Effects of Le on volume fraction profiles.

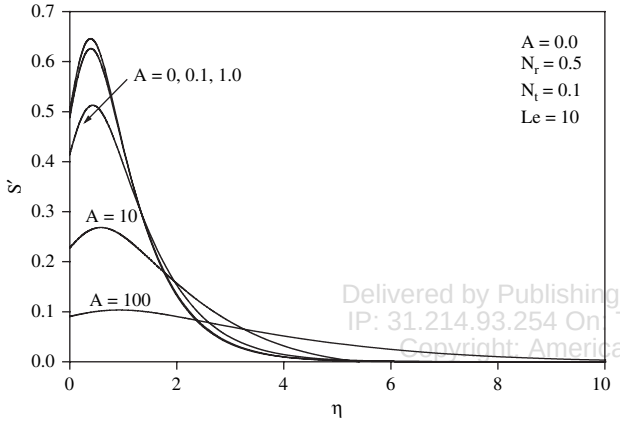

Fig. 14. Effects of A on velocity profiles.

observe that as Le increases, the temperature and concentration within the boundary layer decrease and the thermal and concentration boundary later thicknesses decrease. Figures 14–16 indicate that as the non-Darcy parameter A increases, the velocity increases whereas the temperature and concentration within the boundary layer decrease.

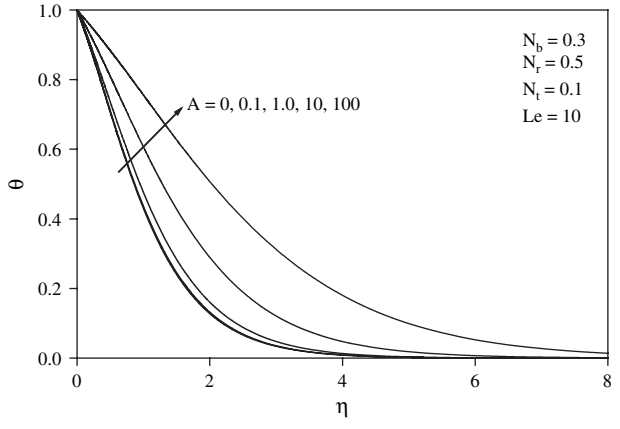

Fig. 15. Effects of A on temperature profiles.

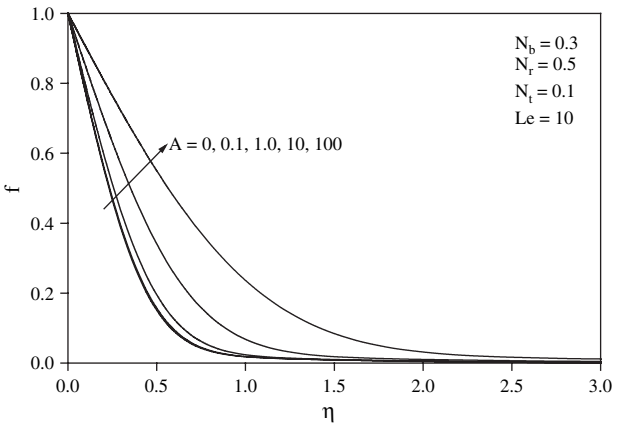

Fig. 16. Effects of A on volume fraction profiles.

4. CONCLUDING REMARKS

In this paper, we presented a boundary layer analysis for the natural convection past a vertical cone embedded in a porous medium saturated with a nanofluid. Numerical results for friction factor, surface heat transfer rate and mass transfer rate have been presented for parametric variations of the buoyancy ratio parameter N_r, Brownian motion parameter N_b, thermophoresis parameter N_t and Lewis number Le. The results indicate that as N_r and N_t increase, the friction factor increases whereas the heat transfer rate (Nusselt number) and mass transfer rate (Sherwood number) decrease. As N_b increases, the friction factor and surface mass transfer rates increase whereas the surface heat transfer rate decreases. As Le increases, The heat and mass transfer rates increase. As the non-Darcy parameter A increases, the heat and mass transfer rates decrease.

NOMENCLATURE

- A Non-Darcy parameter
- D_B Brownian diffusion coefficient
- D_T Thermophoretic diffusion coefficient
- f Rescaled nano-particle volume fraction
- g Gravitational acceleration vector
- k_m Effective thermal conductivity of the porous medium
- K Permeability of porous medium
- Le Lewis number
- N_r Buoyancy Ratio
- N_b Brownian motion parameter
- N_t Thermophoresis parameter
- Nu Nusselt number
- P Pressure
- q'' Wall heat flux
- Ra_x Local Rayleigh number
- r Radial coordinate from the center of the cone
- S Dimensionless stream function

T Temperature
T_W Wall temperature at vertical cone
T_∞ Ambient temperature attained as y tends to infinity
U Reference velocity
u, v Velocity components
(x, y) Cartesian coordinates.

Greek Symbols

α_m Thermal diffusivity of porous medium
β Volumetric expansion coefficient of fluid
ε Porosity
η Dimensionless distance
θ Dimensionless temperature
μ Viscosity of fluid
ρ_f Fluid density
ρ_p Nano-particle mass density
$(\rho c)_f$ Heat capacity of the fluid
$(\rho c)_m$ Effective heat capacity of porous medium
$(\rho c)_p$ Effective heat capacity of nano-particle material
τ Parameter defined by Eq. (13)
ϕ Nano-particle volume fraction
ϕ_W Nano-particle volume fraction at vertical cone
ϕ Ambient nano-particle volume fraction attained
ψ Stream function.

References and Notes

1. J. A. Eastman, S. U. S. Choi, S. Li, W. Yu, and L. J. Thompson, *Appl. Phys. Lett.* 78, 718 (**2001**).
2. S. U. S. Choi, Z. G. Zhang, W. Yu, F. E. Lockwood, and E. A. Grulke, *Appl. Phys. Lett.* 79, 2252 (**2001**).
3. H. E. Patel, S. K. Das, T. Sundararajan, A. Sreekumaran, B. George, and T. Pradeep, *Appl. Phys. Lett.* 83, 2931 (**2003**).
4. S. M. You, J. H. Kim, and K. H. Kim, *Appl. Phys. Lett.* 83, 3374 (**2003**).
5. P. Vassallo, R. Kumar, and S. D'Amico, *Int. J. Heat Mass Transfer* 47, 407 (**2004**).
6. P. Cheng and W. J. Minkowycz, *J. Geophysics. Res.* 82, 2040 (**1977**).
7. R. S. R. Gorla and R. Tornabene, *Transport in Porous Media Journal* 3, 95 (**1988**).
8. R. S. R. Gorla and A. Zinolabedini, *Transactions of ASME, Journal of Energy Resources Technology* 109, 26 (**1987**).
9. W. J. Minkowycz, P. Cheng, and C. H. Chang, *Numerical Heat Transfer* 8, 349 (**1985**).
10. P. Ranganathan and R. Viskanta, *Numerical Heat Transfer* 7, 305 (**1984**).
11. D. A. Nield and A. V. Kuznetsov, *Int. J. Heat Mass Transfer* 52, 5792 (**2009**).
12. D. A. Nield and A. V. Kuznetsov, *Int. J. Heat Mass Transfer* 52, 5796 (**2009**).
13. M. Kumari and S. Jayanthi, *Journal of Porous Media* 8, 73 (**2005**).
14. M. Kumari and G. Nath, *Int. J. Heat Mass Transfer* 52, 3064 (**2009**).
15. N. Prabhat, J. Buongiorno, and L. W. Hu, *J. Nanofluids* 1, 55 (**2012**).
16. S. M. S. Murshed and C. A. N. Castro, *J. Nanofluids* 1, 180 (**2012**).
17. S. M. S. Murshed, C. A. N. D. Castro, and M. J. V. Lourenco, *J. Nanofluids* 1, 175 (**2012**).
18. H. Calvin, P. J. Li, and G. P. Peterson, *J. Nanofluids* 2, 20 (**2013**).

ARTICLE